EARTH SCIENCES
RESEARCH JOURNAL

Earth Sci. Res. J. Vol. 13, No. 2 (December 2009): 108-118

CHARACTERIZATION OF VERMICULITE BY XRD AND SPECTROSCOPIC TECHNIQUES

A. Campos, S. Moreno, R. Molina[1]

[1] *Estado sólido y catálisis ambiental, Departamento de Química, Facultad de Ciencias, Universidad Nacional de Colombia. AK 30 No. 45-03, Bogotá, Colombia; Fax: 57-1-3165220*
E-mail Autor:ramolinag@unal.edu.co

ABSTRACT

A natural mineral from Santa Marta-Colombia used as the starting material in the synthesis of pillared clays has been characterized by several techniques, including X-ray diffraction, X-ray fluorescence, electronic paramagnetic resonance, aluminum nuclear magnetic resonance and scanning electron microscopy. The information revealed that the mineral corresponds to trioctahedral vermiculite. The identification of this mineral is valuable in the control of reduction charge and pillaring processes on these materials to obtain more complex solids like the ones required to specific catalytic applications.

Key words: Vermiculite, structural formula, layer charge.

RESUMEN

Un mineral natural de la región de Santa Marta en Colombia, el cual usado como el material de partida en la síntesis de arcillas pilarizadas, ha sido caracterizado por diversas técnicas tales como difracción de rayos-X, fluoresencia de rayos-X, resonancia electrónica paramagnética, resonancia magnética nuclear de aluminio y microscopía electrónica de barrido. La información en conjunto indica que el mineral corresponde a vermiculita trioctaédrica. La identificación de este mineral es muy importante en la comprensión y el control de los procesos de reducción de carga y de pilarización de estos materiales para la obtención de sólidos más complejos, como los requeridos en aplicaciones catalíticas específicas.

Palabras clave: Vermiculita, fórmula estructura, capa de carga.

1. Introduction

Vermiculite is a clay mineral usually of secondary origin due to the alteration of mica, pyroxene, chlorite or similar minerals (Brown 1961).

The substitutions of Si by Al in tetrahedral sheet predominate in vermiculite. In this way, the negative charge generated on the tetrahedral sheets limits the expansion properties of the clay and this factor determines the high layer staking of its structure (Mac Ewan and Wilson 1980; Tunega et al. 2003).

Manuscript received: 24/03/2009
Accepted for publication: 26/05/2009

From the catalytic point of view, the vermiculite is a very attractive material due to the thermal resistance (Suvorov and Skurikhin 2003) and the number of tetrahedral substitutions, which ensure the presence of a larger number of Brønsted-type acid sites (del Rey-Pérez-Caballero and Poncelet *et al.* 2000); these substitutions are less numerous in other hydrous 2:1 minerals such as smectites. On the whole, these properties offer considerable interest in the production of pillared clays, which are distinguishable from an intercalated layered solid due to their micro and/or mesoporosity and high thermal stability with preservation of the layer stacking (Moreno *et al.* 1997, Schoonheydt *et al*. 1999; Stefanis *et al.* 2006).

The development of pillared clays from vermiculite during the past few years has offered particular interest especially as a heterogeneous catalyst in acid-catalyzed reactions (Campos *et al*. 2005; Campos *et al.* 2007; Campos and Gagea *et al.* 2008; Campos and Moreno *et al.* 2008; Cristiano *et al.* 2005; del Rey-Pérez-Caballero and Poncelet *et al*. 2000; del Rey-Pérez-Caballero and Sánchez *et al*. 2000, Hernández *et al*. 2007). However, as direct intercalation of vermiculite is impossible due to a very high potential of stabilization of interlayer cations (Suvorov and Skurikhin 2003) it has been necessary to develop alternative methodologies to achieve pillared vermiculite (Cristiano *et al*. 2005; F. del Rey-Pérez-Caballero 2000).

One of these methodologies has been the hydrothermal treatment prior to a conventional process of intercalation, in order to reduce negative charge and make possible the subsequent cationic exchange (Cristiano *et al*. 2005). The catalytic profile of Al and Al-Zr modified vermiculites by means of this methodology has confirmed the potential expected for this acidic acid solid, since they are highly active with respect to other clays in alkane hydroisomerization (Campos 2005; Campos *et al.* 2007; Campos and Gagea *et al*. 2008; Campos and Moreno *et al.* 2008; Cristiano *et al.* 2005; del Rey-Pérez-Caballero and Poncelet 2000; del Rey-Pérez-Caballero and Sánchez *et al*. 2000; Hernández *et al.* 2007).

In order to produce practical information to control the modification processes described previously, to achieve a clay mineral with potential catalytic and adsorptive properties, this paper focuses on the characterization of natural vermiculite issued from a Colombian deposit. X-ray diffraction (XRD) and several spectroscopic techniques such as electronic paramagnetic resonance (EPR) and nuclear magnetic resonance (NMR) were used.

2. Experimental

2.1 Materials

The vermiculite selected for this work was labeled V, and it corresponds to a commercial mineral, which comes from a natural deposit in the Santa Marta region in Colombia. Its characterization was carried out with the fraction of a particle size smaller than 150 μm, separated from the commercial form by sieve, without purification or fractioning treatment.

2.2 Characterization methods

The cationic exchange capacity was determined on the clay previously interchanged with an ammonium acetate solution, by means of the micro-Kjeldahl method (Chapman 1965).

The X-ray diffraction study obtained from flakes, which had been gently pressed onto the plates by using a Philips PW 1820 diffractometer (Kα radiation of Cu , λ=1.54056 Å, 40 mA, 40 kV) in 2θ geometry and Bragg–Brentano configuration, a step size of 0.05 and a step time of 2 s. Diffraction patterns were taken at room temperature, 20 °C and 65% of humidity on the average.

The identification of the mineral was assessed according to the position of basal reflection 001 in three patterns: *i)* natural sample, *ii)* after solvation in the presence of ethylene glycol for 24h and *iii)* after heating at 500 ºC for 2 h. In addition, Mg^{2+} and K^{+} saturations were performed in the mineral to achieve a better characterization (Thorez 1976).

Adsorption-desorption isotherms of nitrogen at the temperature of liquid nitrogen were analyzed using a Micromeritics Tristar 3000 instrument on samples previously degassed at 200 °C for 6 h.

Scanning electron microscopy images were recorded in a Philips Scanning Electron Microscope XL30 FEG.

The gravimetric and differential thermal-analysis were performed at a heating speed of 10 ºC min^{-1} in air atmosphere using a Thermal Analyzer TG and DSC Rheometric instruments.

The chemical analysis was performed by X-ray fluorescence in an XRF 2400 instrument. In addition, the Fe^{2+} analysis was carried out through the analytic method described in Wilson M. (Wilson 1995).

Electron paramagnetic resonance spectra in the X band (9.8 GHz) was carried out in a Brucker ESP 3220 spectrometer adopting a modulation frequency of 100 kHz whose

width was fixed at 0.4 mT for wide lines and reduced to 0.05 mT for acute bands, at a temperature of 100 K.

The nuclear magnetic resonance of ^{27}Al was performed in a Brucker Advance 400 spectrometer; the sample was placed in 2.5mm rotors, while 1200 scannings were accumulated with a time of 100ms of recycle. Rotor speed was 5000 Hz.

XRF, EPR and NMR measurements were done additionally in the mineral washed with nitric acid 0.01 M (10 ml g^{-1} clay) by 1h at 30 °C.

3. Results and discussion

3.1 X-ray fluorescence (XRF) and cation exchange capacity (CEC)

Table 1 records the chemical composition of the mineral obtained by X-ray fluorescence. The structural formula of the Colombian vermiculite estimated from its chemical composition and following the methodology described in Wilson M. (Wilson 1995) is:

$$[(Si_{3.04}Al_{0.92}Ti_{0.04})(Al_{0.11}Fe^{3+}_{0.35}Fe^{2+}_{0.07}Mg_{2.41}Mn_{0.003})O_{10}(OH)_2]$$
$$Ca_{0.21}K_{0.05}Na_{0.10}$$

On the other hand, the cationic exchange carried out with ammonium-vermiculite is 1.10 meq $NH_4^+\ g^{-1}$.

3.2 X-ray diffraction analysis

Table 2 shows the comparison between the reflections in XRD for Mg-vermiculite (Brown 1961), those corresponding to a diffraction pattern calculated using DIFK software (Wiewióra *et al.* 2003) and the reflections observed in the pattern for natural vermiculite V.

This parallel makes it possible to observe an analogue pattern between the clays; thus the clay mineral under study corresponds to vermiculite (Wiewióra *et al.* 2003). Likewise, a high layer stacking is highlighted, which is verified by the presence of reflections in series 02*l* and 11*l* (Wiewióra *et al.* 2003).

Reflection 060 located in 0.154 nm indicates that the vermiculite structure is of the trioctahedral type (Dixon and Weed 1989). In general, vermiculite can be dioctahedral or trioctahedral, but trioctahedral type is common in soils with a similar morphology to that of mica (Moore and Reynolds 1997), as observed in vermiculite (Figure 3).

On the other hand, 6th, 8th, and 10th order reflections located at 0.480, 0.360 and 0.288 nm respectively show a growing intensities serie typical for vermiculites (Wiewióra *et al.* 2003). Interstratified material is absent; otherwise the sequence should be abnormal (Wiewióra *et al.* 2003).

Trioctahedral vermiculites usually formed by the weathering of biotite (Gordeeva *et al*. 2002) may be found in the company of this mineral and also talc is possible. In the case of clay V we can suggest that talc is found as a non significant impurity, indicated by its characteristic diffractions in 0.93 nm, 0.48 nm and 0.31 nm (Fagel *et al*. 2001) (Figure 1). In parallel, starting from the positions of reflections 001 and 004 it can be estimated that the vermiculite is found in a proportion larger than 90 % (Thorez 1976).

In order to verify the purity of the mineral, Table 3 records the follow up on reflection 00l of raw natural clay powder, when the sample is solvated in the presence of ethylene glycol and, when the latter is calcined at 500 ºC. This table shows that the V material exhibits the sequence typical of vermiculites (Thorez 1976; Dixon and Weed 1989).

However different authors (Thorez 1976, Dixon and Weed 1989, Malla and Douglas 1987) suggest complementary analysis XRD in Mg^{2+} and K^+-vermiculite to distinguish between soil vermiculites and OH-interlayer vermiculites. As well they suggest a relation between the d_{001} signal and the layer charge.

After saturation with magnesium followed by glycerol the basal reflection should be located in 1.4 nm compared with 1.8 nm if the clay 2:1 were a smectite (Thorez 1976; Fagel et al. 2001). In this sense, the basal reflection of V located at 1.4 nm was not modified. The impossibility for expansion in Mg-V is then a consequence of the strong retention of magnesium between layers with a high negative

Table 1. Chemical composition of Colombian vermiculite.

Oxide	Al_2O_3	SiO_2	Fe_2O_3	FeO	MgO	MnO	CaO	K_2O	Na_2O	TiO_2
%	13.06	45.40	6.91	1.24	24.10	0.11	2.88	0.60	0.26	0.73

Table 2. XRD patterns of Mg-vermiculites, for simulated pattern and the pattern of Colombian vermiculite.

hkl	V	Reference (nm)	
	(nm)	1a	2b
002	1.430	1.44	1.43
004	0.719	0.718	
006	0.480	0.479	0.477
020	0.468	0.460	0.460
008	0.360	0.360	0.358
115	0.339		0.341
0010	0.288	0.287	0.287
200	0.265	0.265	0.264
132	0.259	0.260	0.258
202	0.254	0.255	0.254
204, 0012	0.240	0.238	0.239
136	0.221	0.227	
138, 206	0.206	0.209	
208		0.201	
20î2, 1310	0.187		
2010	0.185	0.184	
0016, 20î4	0.179	0.174	
2012	0.168	0.167	
1314, 20$\bar{1}$6	1.580	0.158	
060	0.154	0.154	0.154
062, 330			0.153
20$\bar{1}$8, 0020	0.144	0.144	
338	0.136	0.136	

a Mg-vermiculite macroscopic of West Chester (Brown 1961).

b Simulated pattern (Wieióra *et al.* 2003).

Table 3. Identification of vermiculite from the basal reflection 001 (nm).

Clay Mineral	N	EG	500
Vermiculite	1.4	1.4	0.96-1.0
Smectite	1.2-1.5	1.7	1.0
Chlorite	1.4	1.4	1.4
V	1.4	1.4	1.0

Natural clay (N), after solvation treatment with ethylene glycol (EG) and the latter heated at 500ºC (500).

density like vermiculites (Slade *et al.* 1976, Tunega *et al*. 2003) (Table 4).

Malla and Douglas (Malla and Douglas 1987) established that the saturation with this potassium originates interlayer space reduction in the region between 1.12 -1.20 nm if the charge is lower than 0.57 and, between 1.00 and 1.06 nm when it is at least 0.6.

In this sense, when clay V was saturated in the presence of K^+ the basal spacing of 1.4 nm was reduced to 1.0 nm after dried at room temperature and calcinations of the sample at 500 °C (Table 4). The reduction of interlayer space after potassium saturation, qualitatively indicate that the layer charge must be higher than 0.57 (Malla and Douglas 1987).

In addition, the previous characteristic is a tool for the clear distinction between vermiculite and chlorite, due to the fact that the latter keeps the 001 reflection at 1.4 nm when K-chlorite, while the basal spacing of K-vermiculite is reduced to 1.0 nm (Dixon and Weed 1989). For this reason, the absence of chlorite is verified as a possible impurity in the mineral.

3.3 Thermal analysis

The thermal-gravimetric (TG) and differential (DTA) analysis of vermiculite is presented in the Figure 2 where a total weight loss of 21.1 % is distributed in several regions. In the first one, the dehydration of the clay takes place in two stages: *i)* between 20 and 110 ºC which corresponds to the loss of water physically absorbed on the surface and *ii)* from 110 ºC to 500 ºC, with a weight loss of 14.3 % attributed to the exit of water molecules, which are in contact with the cations in the interlayer region (Pérez *et al*. 2003).

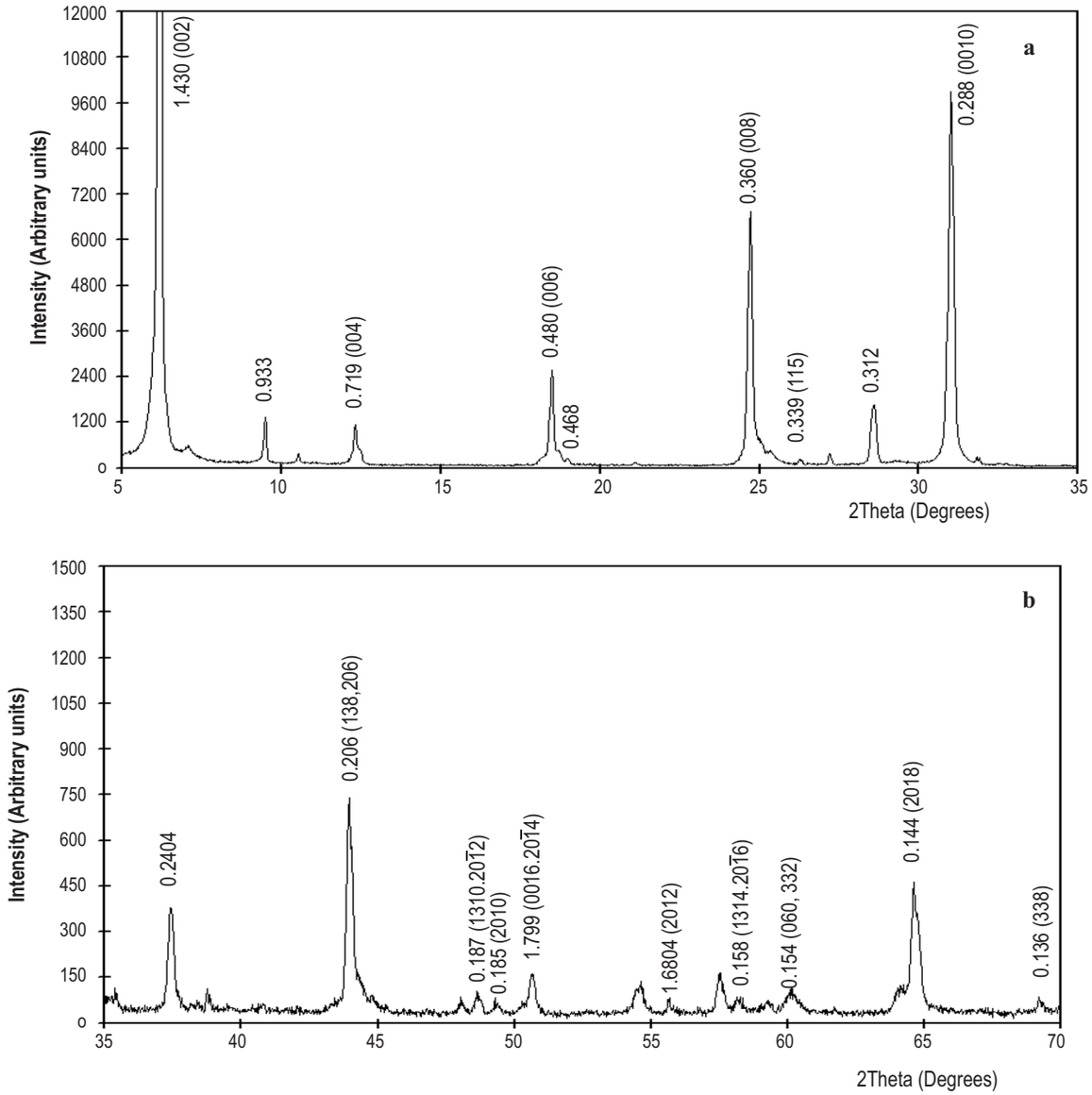

Figure 1. XRD patterns of Colombian vermiculite, in the regions of 5-35 º2θ (a) and 35-70 2θ (b).

Table 4. Comparison of the first order reflection (nm) for high and low charge vermiculites and the Colombian mineral (V).

Vermiculite composition	N	EG	500	Mg_N	Mg_{EG}	K_N	K_{500}
Low charge	1.4	1.6	1.0	1.4	1.6	1.1	1.0
High charge	1.4	1.4	1.0	1.4	1.4	1.0	1.0
V	1.4	1.4	1.0	1.4	1.4	1.0	9.3

Natural vermiculite after Mg^{2+} saturation (Mg_N). Mg_N after solvation with ethylene glycol (Mg_{EG}). Natural vermiculite after K^+ saturation (K_N). K_N heated at 500 ºC (K_{500}).

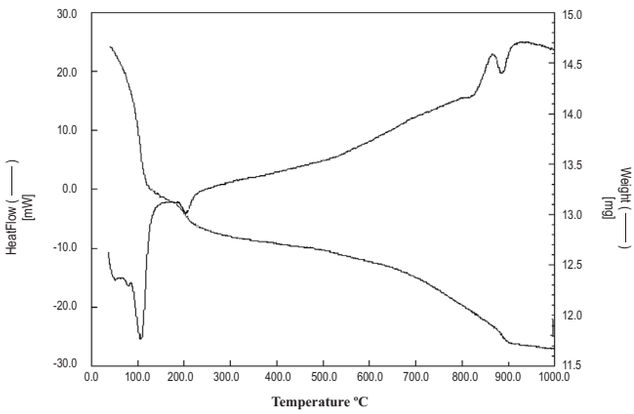

Figure 2. Differential and gravimetric thermal curves of Colombian vermiculite.

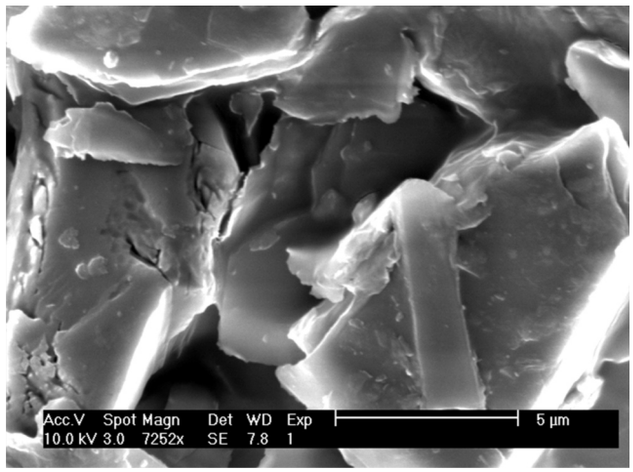

Figure 3. SEM image of vermiculite V.

The region between 500 and 850 ºC records a loss of 6.8 % in weight with a linear tendency with respect to temperature, which is attributed to dehydroxilation (Pérez-Rodríguez *et al*. 2004). In fact, the unusual endothermic peak at 800 °C is associated with the thermal stability on vermiculite which is characteristic of this mineral as well this signal could be assigned to the formation of a new enstatite crystalline phase, which has been reported previously (Pérez *et al.* 2003).

3.4 Texture and morphology

The selected fraction for vermiculite V corresponds to the mineral observed in Figure 3, where large vermiculite layer crystals are detected, which display soft surfaces, with small protuberances. Polygonal sheets with flaked borders are observed in vermiculite formed by the alteration of parental materials (Kishk and Barshad 1969).

The specific surface area (7.41 $m^2 g^{-1}$) corresponding to external surface area without any microporosity. The low surface area is related to the particle but as well with the surface charge, since micas with similar particle size and charge higher than vermiculites have less surface area (del Rey-Pérez-Caballero and Sánchez *et al*. 2000).

The strong hydrogen bonds between the tetrahedral sheet and the water of interlayer cations in vermiculite can keep the interlayer zone obstructed (Tunega D. *et al*. 2003), which could reduce superficial nitrogen adsorption considerably.

By other hand, the relation observed between the interchange cations and the penetration in the interlayer space has been indicated by different authors (Pérez *et al*. 2003). In fact, when monovalent cations in the interlayer region are replaced by those of divalent type, a significant reduction in the superficial area for this mineral clay is observed (Pérez *et al.* 2003).

3.5 Electronic paramagnetic resonance (EPR) and nuclear magnetic resonance of aluminum (^{27}Al-NMR)

Natural vermiculite can be accompanied by iron oxides and hydroxides on its surface (iron that is not substituting aluminum in the octahedral sheet), which will cause an overestimation of iron in vermiculite if it is evaluated by chemical analysis. In this way, EPR could be used to determine the presence of structural Fe^{3+} in vermiculite. Additionally, to evaluate the structural environment of paramagnetic ions found in the clay.

As can be observed in Figure 4, the EPR of V is dominated by signals associated with Fe^{3+} g = 4.3 and 2.1. In addition, a sextet of lines in g = 2 can be appreciated, which is typical of Mn^{2+} species with distorted octahedral symmetry (Tus¡ar *et al*. 2005).

The signal at g = 4.3 is related with Fe^{3+} located at an orthorhombic environment within the clay structure (Bensimon et al. 2000). In general, smectites exhibit signals for Fe^{3+} between g = 4.3 and g = 2.0, which can be attributed to the combination of two different octahedral and two tetrahedral environments. Their formation depends on the possible organizations of the OH groups in the $FeO_4(OH)_2$ unit (Wilson 1995).

Mc Bride et al. (Mc Bride *et al.* 1975) suggest that the difference between the two octahedral sites occupied by

Fe^{3+} ions depends on the nature of the adjacent octahedral cation (divalent or trivalent). According to Timofeeva et al. (Timofeeva *et al.* 2005), the iron found in the form of aggregates in the surface is related with signals in the region comprised between g = 2.3-2.6. Alternatively, different contributions to the wide signal located around g = 2.1 are related with Fe_xO_y or FeOOH species (Chung *et al*. 2004).

In the case of the smectite minerals the signal at g = 4.3 is assigned to the presence of isolated Fe^{3+} in tetrahedral or octahedral coordination, which corresponds to the iron located in the interior of the clay sheets (iron substituting aluminum in the octahedral layers). On the other hand, the signal at g = 2.0 is associated to the presence of clusters of iron (iron extra-red species) (Carriazo *et al.* 2005).

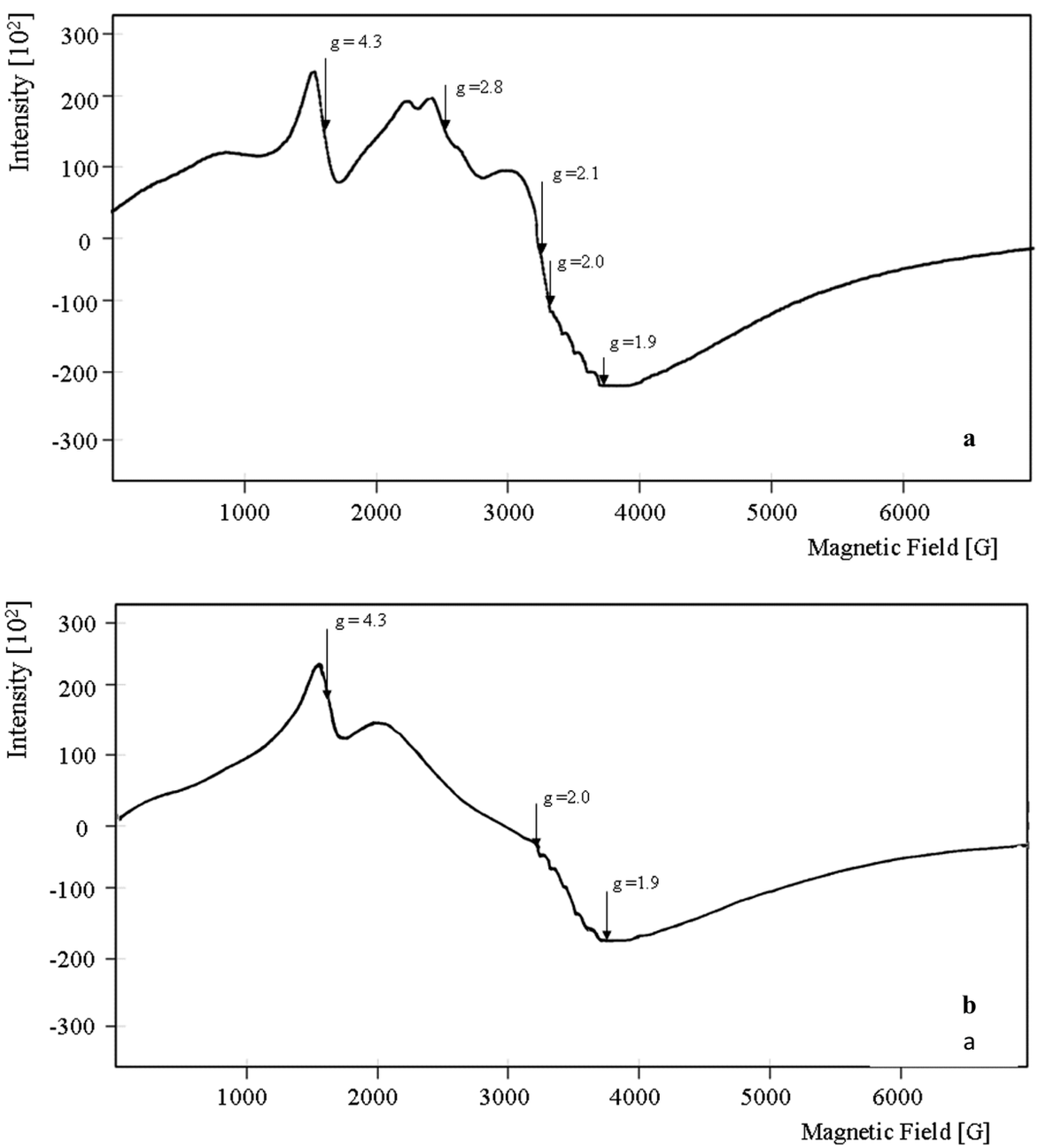

Figure 4. EPR spectra of Colombian vermiculite at 100 K. (a) Natural mineral, (b) natural mineral after mild acid treatment.

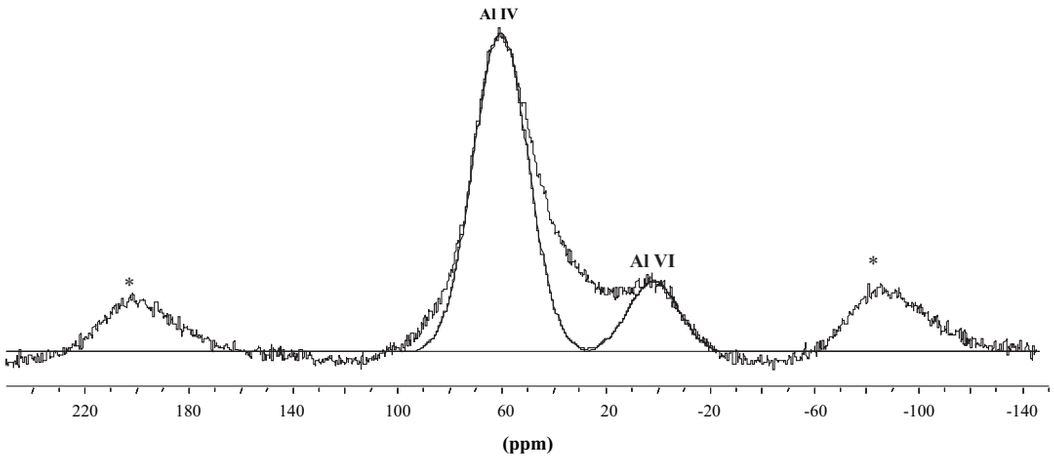

Figure 5. ^{27}Al MAS-NMR spectra of the Colombian vermiculite. (*) Spinning sidebands.

As observed in Figure 4a, several signals point to the presence of iron extra-red species on the surface of the clay V. For this reason, the clay was submitted to a soft acid wash to remove impurities from its surface. In Figure 4b, the absence of signals between g = 2.3-2.6 indicates that these species had been removed.

Likewise, signals of Mn^{2+} ions located in the region at g = 2, and g = 1.9 (Figure 4a), and the multiple signal recorded is interpreted in terms of the interaction between structural ions Mn^{2+} and Fe^{3+} and other environments (Kessissoglou 1999). After acid wash Mn^{2+} signals remain invariable which suggest structural positions for this cation.

Respect to aluminum, in order to evaluate the structural environment as well as the AL(IV)/AL(VI) ratio to compare with the ratio estimated in the structural formula, ^{27}Al MAS-NMR spectra was made. The spectrum is shown in Figure 5, in which an intense signal at 60 ppm is observed (with two sidebands at -60 and 190 ppm). This signal is associated with Al(IV) substituting the silica in the tetrahedral sheets (Klinowski 1999). A second signal corresponding to Al(IV) at 0 ppm (Klinowski 1999) was observed. The intensity ratio Al (IV)/ Al (VI) was 10.4.

3.6 Correlation of Results

Weaver (Weaver 1958) suggested that vermiculite derived from mica weathering has a high laminar charge and its 001 reflection decrease to 1.0 nm after potassium saturation, as happens in clay V (Table 4). In contrast, vermiculites generated by the weathering of materials like amphiboles or volcanic material exhibit a limited layer contraction with the same treatment.

In fact, the laminar charge is a fundamental element in identification of 2:1 silicates. In fact, the AIPEA (International Association for the Study of Clays) established that vermiculite is a phylosilicate 2:1 with a charge of 0.6 to 0.9 per unit cell (Guggenheim et al. 2006). In this sense, to determine the layer charge of V, it was performed with the structural formula, which was determined through XRF elemental analysis. In it formula can be deduced that the tetrahedral sheet originate an excess negative charge of -0.9 e/ $O_{10}(OH)_2$, which is compensated by Ca^{2+}, Na^{+} and K^{+} cations. As regards to the octahedral sheet, formed specially by Fe^{3+} and Mg^{2+} it carries a positive charge of 0.35, resulting in a total negative charge of 0.6 e- / $O_{10}(OH)_2$.

In order to confirm the approach to the elemental organization and to evaluate the environment of the elements found in the structure, EPR and NMR provide very valuable information. Thus, by means of EPR spectroscopy, iron species on the natural clay surface were detected, which can be easily removed through a soft acid wash (Figure 4b). In consequence, the chemical analysis by XRF to evaluate the structural formula was done in the mineral washed with soft acid because unwashed sample could overestimate the iron content.

Regarding the NMR the Al (IV)/Al (VI) ratio (10.4) compared with the ratio estimated with the structural formula (8.9) is a satisfactory approach of vermiculite structure take into account that paramagnetic species such as iron can modify the tetrahedral/octahedral ratio (Gates *et al.* 1996).

The total negative charge (Malla and Douglas 1987; Guggenheim et al. 2006) observed in the structural formula and the slight difference with the CEC as well as the XRD signals and the follow up of the basal reflection 001 after submitting the sample to different treatments (Thorez 1976;

Wilson 1995; Moore and Reynolds 1997) indicate that mineral V is trioctahedral vermiculite.

The knowledge derived from the present work is very useful in further understanding, controlling and predicting the modifications that can be performed on this attractive natural mineral in order to obtain materials with technological impact such as catalyst and adsorbents (Campos *et al*. 2005; Cristiano et al. 2005; Campos *et al*. 2007; Campos and Gagea *et al.* 2008; Campos and Moreno *et al.* 2008, Hernández *et al.* 2007).

5. Conclusion

Mineral clay from a deposit in the region of Santa Marta, Colombia has been characterized through different techniques. The correlation of results indicates that the mineral corresponds to trioctaheral vermiculite as result of the mica-biotite weathering process. The layer stacking, its high thermal stability, low superficial area and the magnitude of its negative charge are characteristic of vermiculite. The details about the structure of this mineral are highly useful in the latter pillaring process of these mineral to enhance their catalytic applications.

Acknowledgements

This research has been supported by Projects Code HERMES 9887 VRI-DIB-Universidad Nacional de Colombia. The authors wish to thank Professor Pierre Jacobs, director of the Centrum voor Oppervlaktechemie en Katalyse at Katholieke University of Leuven for carrying out the NMR and EPR analysis.

References

Bensimon Y., Deroide B., Dijoux F., Martineau M. (2000). Nature and thermal stability of paramagnetic defects in natural clay: a study by electron spin resonance. *Journal of Physics and Chemistry of Solids* **61**, 1623-1632.

Brown B. (1961) *The X-Ray identification and crystal structures of clay minerals*. Mineralogical Society; London.

Campos A., Moreno S., Molina R. (2005). Acidez e hidroisomerización de heptano en una vermiculita colombiana modificada con aluminio. *Revista Colombiana de Química*. **34**, 79-92.

Campos A., Gagea B., Moreno S., Jacobs P., Molina R. (2007). Hydroisomerization of decane on Pt/Al,Ce-pillared vermiculites. *Studies in Surface Science and Catalysis*. **170,** 1405-1409.

Campos A., Gagea B., Moreno S., Jacobs P., Molina R. (2008). Decane hydroconversion with Al-Zr, Al-Hf, Al-Ce-pillared vermiculites. *Applied Catalysis A*. **345,** 112-118.

Campos A., Moreno S., Molina R. (2008). Relationship between hydrothermal treatment parameters as a strategy to reduce layer charge in vermiculite, and its catalytic behavior. *Catalysis Today.* **133-135,** 351-356.

Carriazo J., Guélou E., Barrault J., Tatibouët J., Molina R., Moreno S., 2005. Synthesis of pillared clays containing Al, Al-Fe or Al-Ce-Fe from a bentonite: Characterization and catalytic activity. *Catalysis Today* **107–108,** 126–132.

Chapman H. (1965). Cation exchange capacity. In: Black C, Evans D, White J, Ensminger L, Clark E, editors. *Methods of Soil Analysis (Agronomy 9),* American Society of Agronomy.

Chung H., Sang-Won C., Yong-Sik O., Jinho J. (2004). EPR characterization of the catalytic activity of clays for PCE removal by gamma-radiation induced by acid and thermal treatments. *Chemosphere* **57**, 1383-1387.

Cristiano D., Campos A., Molina R. (2005). Charge reduction in a vermiculite by acid and hydrothermal methods: A comparative study. *Journal of Physical Chemistry B* **109,** 19026-19033.

del Rey-Pérez-Caballero F., Poncelet G. (2000). Microporous 18 Å Al-pillared vermiculites: preparation and characterization. *Microporous and Mesoporous Materials*. **37,** 313-327.

del Rey-Pérez-Caballero F., Sánchez M., Poncelet G. (2000). Hydroisomerization of octane on Pt/Al-pillared vermiculite, and comparison with zeolites. *Studies in Surface Science and Catalysis*. **130,** 2417-2422.

Dixon J., Weed S. (1989). *Minerals in soil environments*. Second edition. United States.

Fagel N., Robert C., Preda M., Thorez J. (2001). Smectite composition as a tracer of deep circulation: the case of the Northern North Atlantic. *Marine Geology*. **172,** 309-330.

Gates W., Stucki J., Kirkpatrick R. (1996). Structural properties of reduced Upton montmorillonite. *Physics and Chemistry of Minerals* **2,** 535-541.

Gordeeva L., Moroz E., Rudina N., Aristov Y. (2002). Formation of porous vermiculite structure in the course of swelling. *Russian Journal of Applied Chemistry*. **75,** 357-361.

Guggenheim S., Adams J., Bain B., Bergaya F., Brigatti M., Drits V., Formoso M., Galán E., Kogure T., Stanjek H. (2006). Summary of recommendations of nomenclature committees relevant to clay mineralogy: report of the association international pour l'etude des argiles (AIPEA) nomenclature committee for 2006. *Clays and Clay Minerals*. **54,** 761-772.

Hernández W., Centeno M., Odriozola J., Moreno S., Molina R. (2007). Acidity characterization of a titanium and sulfate modified vermiculite. *Materials Reserach Bulletin*. **43,** 1630-1640.

Kessissoglou D. (1999). Homo- and mixed-valence EPR -active trinuclear manganese complexes. *Coordination Chemistry Review*. **185,** 837-858.

Kishk F., Barshad I. (1969). The morphology of vermiculite clay particles as affected by their genesis. *American Mineralogist*. **54,** 849-857.

Klinowski J. (1999). Solid-state NMR studies of molecular sieve catalysts. *Chemical Reviews*. **91,** 1459-1479.

Laird D. (1999). Layer Charge Influences on the Hydration of Expandable 2:1 Phyllosilicates. *Clays and Clay Minerals*. **47,** 630-636.

Malla P., Douglas L. (1987). Layer charge properties of smectites and vermiculites: tetrahedral vs. Octahedral. *Soil Science Society of America Journal*. **51,** 1362-1366.

MacEwan, D. and Wilson, M. (1980). Interlayer and intercalation complexes of clay minerals. Pp. 197 248 in: *Crystal Structures of Clay Minerals and Their X-ray Identification* (G.W. Brindley and G. Brown, editors). Mineralogical Society, London.

Mc Bride M., Pinnavaia T., Mortland M. (1975). Exchange Ion Positions in Smectite: Effects on Electron Spin Resonance of Structural Iron. *Clays and Clay Minerals*. **23,**162-164.

Moreno S., Gutiérrez E., Alvarez A., Papayannakos N., Poncelet G. (1997). Al-pillared clays: from lab syntheses to pilot scale production characterization and catalytic properties. *Applied Catalysis A* **165,** 103-114.

Moore D., Reynolds J. (1997) . X-*ray diffraction and the identification and analysis of clay minerals*. Second edition. Oxford university press.

Pérez L., Balek V., Potayo J., Pérez J., Subrt J., Bountsewa I., Beckman I., Málek Z. (2003). Study of natural and ion exchanged vermiculite by emanation thermal analysis, TG, DTA and XRD. *Journal of Thermal Analysis and Calorimetry*. **71**, 715-726.

Pérez-Rodriguez J., Potayo J., Jiménez de Haro M., Pérez-Maqueda L., Lerf A. (2004). Thermal decomposition of NH_4^+-vermiculite from Santa Olalla (Huelva, Spain) and its relation to the metal ion distribution in the octahedral sheet *Physics and Chemistry of Minerals* **31,** 415-420.

Schoonheydt R., Pinnavaia T., Lagaly G., Gangas N. (1999). Pillared clays and pillared layered solids. *Pure Applied Chemistry*. **71**: 2367-2371.

Slade P. (1976). Telleria M., Radoslovic W. The estructures of ornithine-vermiculite and 6-aminohexanoic acid-vermiculite. *Clays and Clay Minerals* **24,** 134-141.

Suvorov D., Skurikhin V. (2003). Vermiculite: A promising material for high-temperature heat insulators. *Refractories and Industrial Ceramics*. **44,** 186-193.

Stefanis A., Tomlinson A. (2006). Towards designing pillared clays for catalysis. *Catalysis Today* **114**, 126-141.

Thorez J. (1976). *Practical identification of clay minerals*. G. Lelotte (Ed). Dison, Belgique.

Timofeeva M., Khankhasaeva S., Badmaeva S., Chuvilin A., Burgina E., Ayupov A., Panchenko V., Kulikova A. (2005). Synthesis, characterization and catalytic application for wet oxidation of phenol of iron-containing clays. *Applied Catalysis B*. **59**: 243-248.

Tunega D., Lischka H. (2003). Effect of the Si/Al ordering on structural parameters ad the energetic stabilization of vermiculites- a theoretical study. *Physics and Chemistry of Minerals* **30,** 517-522.

Tus¡ar N., Zabukovec N.,Vlaic G., Arc¡on D., Daneu N., Kauc¡ic¡ V. (2005). Local environment of manganese incorporated in mesoporous MCM-41. *Microporous and Mesoporous Materials*. **82,** 129-136.

Weaver C. (1958). Effects of geologic significance of potassium "fixation" by expandable clay minerals derived from muscovite, biotite, chlorite and volcanic material. *American Mineralogist*. **43,** 839-861.

Wiewióra A., Perez-Rodriguez L., Perez-Maqueda L., Drapala J. (2003). Particle size distribution in sonicated high- ad low charge vermiculites. *Applied Clay Science*. **24**, 51-58.

Wilson M. (1969). *Mineralogy: Spectroscopy and Chemical Determinative Methods*. Champan & Hall ed; London.